Food and Chemical Toxicology 124 (2019) 219–230

Contents lists available at ScienceDirect

Food and Chemical Toxicology

journal homepage: www.elsevier.com/locate/foodchemtox

Antrodia salmonea suppresses invasion and metastasis in triple-negative breast cancer cells by reversing EMT through the NF-κB and Wnt/β-catenin signaling pathway

You-Cheng Hseu[a,b,c], Yi-Chun Lin[d], Peramaiyan Rajendran[a], Varadharajan Thigarajan[d], Dony Chacko Mathew[a], Kai-Yuan Lin[e], Tzong-Der Way[f], Jiunn-Wang Liao[g], Hsin-Ling Yang[d,*]

[a] Department of Cosmeceutics, College of Biopharmaceutical and Food Sciences, China Medical University, Taichung, 40402, Taiwan
[b] Department of Health and Nutrition Biotechnology, Asia University, Taichung, 41354, Taiwan
[c] Chinese Medicine Research Center, China Medical University, Taichung, 40402, Taiwan
[d] Institute of Nutrition, College of Biopharmaceutical and Food Sciences, China Medical University, Taichung, 40402, Taiwan
[e] Department of Medical Research, Chi-Mei Medical Center, Tainan, 710, Taiwan
[f] Department of Life Sciences, College of Biopharmaceutical and Food Sciences, China Medical University, Taichung, 40402, Taiwan
[g] Graduate Institute of Veterinary Pathology, National Chung Hsing University, Taichung, 402, Taiwan

ARTICLE INFO

Keywords:
Antrodia salmonea
Triple-negative breast cancer
Metastasis
EMT
Wnt/β-catenin

ABSTRACT

Antrodia salonea (AS), a fungus that is indigenous to Taiwan has been well known for its anti-cancer properties. We investigated the anti-metastatic and anti-epithelial-mesenchymal transition (EMT) properties of AS in TNBC cells. To determine their EMT and metastasis levels, *in vitro* wound healing, wound invasion, Western blotting, RT-PCR, luciferase activity and immunofluorescence assays were performed, while the *in vivo* anti-metastatic efficacy of AS was evaluated in BALB/c-nu mice through bioluminescence imaging, HE staining, and immunohistochemical staining. MDA-MB-231 cells, when treated with AS concentrations (25–100 μg/mL) resulted in significant reduction of invasion and migration as well as the downregulation of VEGF, uPAR, uPA and MMP-9 (inhibition of PI3K/AKT/NFκB pathways). AS treatment prevented morphological changes and reversed EMT through the upregulation of E-cadherin and the downregulation of N-cadherin, Slug, Twist, and Vimentin. Inhibition of Smad3 signaling pathway, downregulation of β-catenin pathway and upregulation of GSK3β expression were also observed while, suppression of metastasis and EMT in TGF-β1-stimulated non-tumorigenic MCF-10A cells was observed when treated with AS. Histological analysis confirmed that AS reduced tumor metastasis and upregulated E-cadherin expression in biopsied lung tissues. Our results indicated that AS exhibits anti-EMT and anti-metastatic activity, that could contribute to develop anticancer drugs against TNBC.

1. Introduction

The molecular subtype of triple-negative breast cancer (TNBC) encompasses approximately 15%–20% of all diagnoses of invasive breast cancer, and this subtype has the lowest 5-year survival rate among all breast cancer types. TNBC's are aggressive, fast growing subtypes of breast cancer cells that lack Estrogen (ER^-), Progestrone (PR^-) and HER2 ($HER2^-$) receptors, this characteristics make their treatment resistant to hormonal therapy and other treatment methods targeting HER2 receptors (Wahba and El-Hadaad, 2015; Isakoff, 2010). The adverse side effects of the varied breast cancer treatment approaches on healthy cells as well as the tendency of some cancer cells to develop resistance against treatments are problems that need to be addressed (Bao et al., 2017). Epithelial–mesenchymal transition (EMT) plays a pivotal role not only in the metastasis of tumors, but also in the development of drug resistance (Wang et al., 2017), which are characterized by the reduction in E-cadherin (Epithelial marker) and increase in N-cadherin (Mesenchymal marker) levels. Low expression of E-cadherin in breast cancer was associated with taxane residues, which has drug resistance properties (Wang et al., 2017). Studies have determined that nuclear β-catenin accumulation is required for EMT. The cytoplasm β-catenin/E-cadherin complex establishes the epithelial junctions. Disruption in this process results in abnormal cell–cell adhesion and compromised Wnt signaling during metastasis induced by

* Corresponding author. Institute of Nutrition, College of Biopharmaceutical and Food Sciences, China Medical University, 91, Hsueh-Shih Road, Taichung, 40402, Taiwan.
E-mail address: hlyang@mail.cmu.edu.tw (H.-L. Yang).

https://doi.org/10.1016/j.fct.2018.12.009
Received 28 May 2018; Received in revised form 29 November 2018; Accepted 6 December 2018
Available online 07 December 2018
0278-6915/

EMT (Yao et al., 2011). EMT involves AKT/GSK or NFκB-mediated expression of Snail and promotes cell invasion and migration in various cancers, such as breast, colon, and renal cancers (Wang et al., 2013). Maier et al. (2010) determined that when accompanied by sustained NFκB activation, EMT could occur in breast cancer cells, even when TGF-β1 was absent. The enhanced activity of P13K promotes AKT activation and increases NFκB subunit p65 expression. Ras activates the PI3K/AKT signaling pathway; which inturn reactivates NFκB to induce the expression of EMT regulatory proteins, resulting in the down-regulation of E-cadherin expression, leading to EMT-induced metastasis.

Several medicinal mushroom formulations have been assessed for treatment of various forms of cancer (Tang et al., 2008). Furthermore, they have been used in the treatment of several conditions, including abdominal pain, diarrhea, drug intoxication, food poisoning, and hypertension (Tsai, 1985). *Antrodia salmonea* (AS) has been demonstrated to exert myriad of biological effects, including antiangiogenic, anti-atherogenic, anti-inflammatory, anticancer, and antioxidant effects (Chang et al., 2017b; Hseu et al., 2014c, d; Yang et al., 2014, 2015). Previous studies have shown that AS induced apoptosis, autophagy, and cell-cycle arrest in TNBC cells as well as suppressed tumor growth in athymic nude mice (Chang et al., 2017a, b). In this study, the *in vivo* and *in vitro* abilities of non-cytotoxic concentrations (25–100 μg/mL) of AS to inhibit metastasis and EMT of MDA-MB-231 TNBC cells were studied. The molecular signaling links connecting AS and EMT in the metastatic process were also investigated.

2. Materials and methods

2.1. Reagents and antibodies

Sigma-Aldrich (St. Louis, Mo., United States) supplied 3-(4,5-dimethylthiazol-2-yl)-2,5-diphenyltetrazolium bromide (MTT). Gibco Brl/Invitrogen (Carlsbad, Calif., United States) supplied fetal bovine serum (FBS), $_L$-glutamine, and Dulbecco's modified Eagle's medium (DMEM) as well as streptomycin, penicillin, and neomycin. Antibodies to uPA, uPAR, β-catenin, Vimentin, Twist, β-actin, E-cadherin, and VEGF were sourced from Santa Cruz Biotechnology (Heidelberg, Germany). Antibodies to MMP-9, NFκB (p65), p-PI3K, PI3K, p-AKT, AKT, GSK3β, p-β-catenin, histone H3, p-Smad3, Smad3, p-Smad2, Smad2, and p-GSK3β were acquired from Cell Signaling Technology. (Danvers, Mass., United States). PeproTech supplied TGF-β1 (Rocky Hill, N.J., United States). Antibodies to N-cadherin and Slug were obtained from GeneTex, Inc. (Irvine, Calif.). The remaining chemicals were procured from Sigma-Aldrich (St. Louis, Mo) or Merck & Co. (Darmstadt, Germany).

2.2. Cell culture

The non-tumorigenic MCF-10A and tumorigenic MDA-MB-231 cell lines were sourced from American Type Culture Collection (ATCC, United States). MDA-MB-231 cells were cultured in DMEM supplemented with penicillin–streptomycin–neomycin (1%), L-glutamine (2 mM), and heat-inactivated FBS (10%) and incubated under standard condition (5% CO_2, 37 °C, 95% humidity), while for the growth of MCF-10A cells, DMEM/F12 was supplemented under the same incubator conditions with glutamine (2 mM), hydrocortisone (0.5 μg/mL), heat-inactivated FBS (10%), insulin (10 μg/mL), penicillin–streptomycin–neomycin (1%), and human epidermal growth factor (20 ng/mL). After harvesting the cultures, the cells were counted using a hemocytometer, and the morphological changes of the cells were characterized through phase-contrast microscopy (magnification: 200 ×).

2.3. Preparation of submerged cultures of Antrodia salmonea

A new species of genus *Antrodia*, *Antrodia salmonea* was isolated from Nantou, Taiwan, identified by Dr. Shy-Yuan Hwang of the Endemic Species Research Institute (Jiji, Nantou), while a voucher specimen (#AS001) was deposited at China Medical University (Taichung City, Taiwan). The AS hyphae and the fruiting bodies were separated, and the entire colony was divided and put in a flask of 50 mL distilled water. The mycelial suspension was incubated post homogenization by using a culture medium, comprising glucose (2.0%), peptone (0.1%), and wheat powder (0.1%) prepared in double distilled water and pH adjusted to 5. Then, the cultures were grown in an Erlenmeyer flask of capacity 2 L that contained the medium (1 L). The cultures were then incubated while subject to shaking (120 rpm, 25 °C, 10 days). Afterward, 3.5 L of the resultant culture was inoculated into a fermenting tank (capacity: 500 L) that contained 300 L of the culture medium and fermented for 30 days at 25 °C, at an aeration rate of 0.075 vvm; this rate was selected to yield a mucilaginous medium that contained the mycelia. A batch of 2–4 fermented AS cultures were used in the experiments. Subsequently, the fermented deep yellow product was concentrated in vacuum to a total dry matter yield of 15 g/L, freeze dried, ground, and shaken with distilled water, followed by the centrifugation at 3000*g* and filter sterilization (0.22-μm filter) of the medium. The aqueous extracts were finally concentrated under vacuum (providing a yield of approximately 0.375 g), freeze-dried, and powdered. The stock solution was prepared by solubilizing the powdered samples using sodium phosphate buffer (10 mM; pH 7.4) that contained NaCl (0.15 M; PBS) at 25 °C. The solution were stored at −20° until further use.

2.4. MTT assay

The MTT colorimetric assay was employed to monitor cell viability. Cells (4×10^5 cells per well) were developed on 12-well cell culture plates to confluency and incubated for 24 h using AS (50–400 μg/mL). These cells were then incubated in PBS by using 400 μL of MTT (0.5 mg/mL) for 2 h. Subsequently, the culture supernatant was removed, and the residual formazan crystals were dissolved in DMSO (400 μL) and the absorbance of the plate was measured at 570 nm through ELISA plate reader (Bio-Tek Instruments, Vt., United States). AS effects on cell viability were evaluated as the proportion of viable cells in relation to the vehicle-treated control cells, which were arbitrarily deemed to be 100%.

2.5. Cell migration assessment using in vitro wound-healing assay

Cell migration was assessed via *in vitro* wound-healing assay. Briefly, cells (1×10^4 cells per well) underwent culturing on Ibidi culture inserts in 12-well 1%-gelatin-coated plates. Afterward, cells were incubated for 24 h in FBS medium using the indicated AS concentration (25–100 μg/mL). The cells subsequently underwent two washes with PBS, after which they were fixed using methanol (100%) and stained using Giemsa Stain solution (Merck & Co.). Optical microscopy (magnification: 200 ×) was employed to photograph the cultures in order to monitor cell migration to the wounded region, whose area was calculated with Image-Pro Plus (Media Cybernetics, Md., United States).

2.6. Cell invasion assay

Cell invasion assays were performed using Matrigel invasion chambers (BD, Mass., United States). 10 μL of Matrigel (25 mg/50 mL) was applied to the polycarbonate membrane filters (pore size 8 μm) and seeded 1×10^5 cells onto filters coated in Matrigel in serum-free medium (200 μL) that contained AS (25–100 μg/mL) in triplicate. Thus, the apparatus' bottom chamber held 750 μL of the complete growth medium. The cells were subsequently left to migrate at 37 °C for 24 h, Following which the cells remaining on the membrane's top surface that did not migrate were removed using a cotton swab. The cells that did migrate through the membrane to its bottom were fixed for 15 min in

cold methanol (75%) and washed with PBS thrice. Afterward, Giemsa Stain solution was employed to stain the cells, and PBS was subsequently used to destain them. Through optical microscopy (magnification: 200 ×) and manual counting, the number of migrating cells was tallied.

2.7. Gelatin zymography assay

The uPA and MMP-9 activities in the medium arising from the MDA-MB-231 cells were evaluated using gelatin zymography protease assays. A cell density of 3×10^5 of MDA-MB-231 cells were seeded and grown in 12-well culture dishes containing DMEM with FBS (10%) to a near-confluent cell monolayer were grown. Subsequently, they were re-suspended in DMEM containing FBS (1%) and incubated with AS (25–100 μg/mL) for 24 h. Briefly, a suitable volume of the collected media (altered to reach viable cell numbers) was synthesized with SDS sample buffer but with neither boiling nor reduction. Thereafter, 1 mg/mL gelatin (casein) for MMPs (uPA) was supplemented, and the mixture underwent SDS-PAGE (8%) electrophoresis. The resultant gels were cleaned using Triton X-100 (2.5%); they subsequently underwent 24-h incubation at 37 °C in a buffer containing Tris-base, 50 mM; NaCl, 200 mM; $CaCl_2$, 5 mM; and Brij 35, 0.02%). Subsequently, Coomassie brilliant blue R-250 was used to stain the gels.

2.8. Extraction of RNA and analysis of RT-PCR

Following pretreatment, the cells were harvested for 24 h using AS at concentrations 25–100 μg/mL. Trizol-Reagent (Invitrogen) was used to prepare the total RNA from the cultured cells. Subsequently, 1 μg total RNA aliquots underwent RT-PCR using a SuperScript-III One-Step RT-PCR platinum *taq* Kit (Invitrogen) and a Bio-Rad iCycler PCR instrument (Bio-Rad); amplification was achieved via 25–40 cycles of denaturing at 95 °C for 30 s and annealing at 60°C–65 °C for 30 s, followed by primer extension for 72 °C at 1 min. The resulting products were stained using ethidium bromide and subjected to electrophoresis in agarose gel (1%). The primer sequences employed in this study were the following: MMP-9 forward, 5′-TTGACAGCGACAAGAAGTGG-3′, reverse, 5′-GCCATTCACGTCGTCCTTAT-3′ (Heo et al., 2010); E-cadherin forward, 5′-TGGGTTATTCCTCCCATCAG-3′, reverse, 5′-TTTGTC AGGGAGCTCAGGAT-3′ (Sehrawat and Singh, 2011); N-cadherin forward, 5′-CACCCAACATGTTTACAATCAACAATTGAGAC-3′, reverse, 5′-CTGCAGCAACAGTAAGGACAAACATCCTATT-3′ (Pai et al., 2013); β-actin forward, 5′-CAAAGACCTGTACGCCAACAC-3′, reverse, 5′-ATACT CCTGCTTGCTGATCC-3′′ (Sehrawat and Singh, 2011).

2.9. Protein isolation and western blot analysis

1×10^6 cells were seeded into each 6-cm dish and subsequently pretreated with AS concentration varying from 25 to 100 μg/mL for 24 h. Following treatment, the cells were detached and rinsed once in cold PBS; subsequently, the cytoplasmic, nuclear, and total extracts were prepared in accordance with the procedures for the extraction reagents (Pierce Biotechnology, Rockford, Ill., United States). The Bio-Rad protein assay was used to determine the protein content in each sample, with bovine serum albumin (BSA) as the standard. SDS-PAGE (8–15%) was used to electrophorese identical amounts (50 μg) of the denatured samples. Subsequently, the proteins were transferred to the PVDF membranes overnight. 5% of skimmed milk was used to block the membranes at room temperature for 30 min and without delay reacted for 2 h using primary antibodies. Following the primary antibody incubation, the PVDF membrane were exposed to horseradish peroxidase–conjugated goat anti-mouse or anti-rabbit secondary antibody for 2 h and subsequently developed further on an enhanced chemiluminescence substrate (Pierce Biotechnology, Rockford, Ill., United States). AlphaEase (Genetic Technology, Miami, Fla., United States), a commercial software package, was used to create a graph of the densitometric band intensities using normalization of the control to 1-fold.

2.10. Luciferase reporter assay

The NFκB, β-catenin, Smad3, and Smad2 transcriptional activities were characterized using a Promega dual-luciferase reporter assay system (Wisconsin., United States). The cells underwent culturing in 24-well plates until they achieved 70%–80% confluence and the cells were incubated in serum-free DMEM containing no antibiotics for 6 h. Further, they were transfected using either NFκB/β-catenin/Smad3 (pGL3-SBE4-Luc reporter vector)/Smad2 (3 TP-Luc) plasmids with β-galactosidase using Lipofectamine 2000 (Invitrogen, Grand Island, N.Y., United States) or a pcDNA vector. Afterward, AS of varying concentration of 25–100 μg/mL was used to treat the cells for 4 or 24 h. Following incubation, cells were lysed and measured for their luciferase activity, normalized to cell lysates' β-galactosidase activity, with a luminometer (Bio-Tek Instruments, Vt.). A luminance ELISA reader was used to quantify the relative fluorescence intensity.

2.11. Immunofluorescence staining

Cells underwent culturing in eight-well glass Tek chambers (density: 1×10^4 cells per well); additionally, they underwent AS (50–100 μg/mL) pretreatment for the indicated times. The cells were fixed in paraformaldehyde (2%) for 15 min, permeabilized using Triton X-100 (0.1%) for 10 min, rinsed, and blocked using FBS (10%) in PBS. Afterward, they underwent 2-h incubation in FBS (1.5%) using anti-β-catenin or anti-p65 primary antibodies. Subsequently, the cells underwent 1-h incubation using a 488 nm FITC–conjugated secondary antibody in BSA (6%). Following the cells were stained for 5 min using 1 μg/mL DAPI, washed using PBS, as well as visualized through confocal laser scanning microscopy (magnification: 400/630 ×).

2.12. Wnt luciferase activity assay

Mouse embryonic carcinoma P19 cells (BCRC No. 60052) were acquired from Bioresource Collection and Research Center, Hsinchu City, Taiwan, and were maintained in minimum essential medium alpha (Gibco, Life technologies, N.Y., United States), supplemented with FBS (2.5%; HyClone, GE Healthcare, Utah, United States), penicillin–-streptomycin (1% Gibco), sodium pyruvate (1 mM; Gibco), and bovine calf serum (7.5%; HyClone). The cells were incubated under the standard conditions (5% CO_2, 37 °C, 95% humidity) and were passaged once every 2 days. Afterward, 1×10^5 P19 cells per well were seeded into a 24-well dish and cultured overnight. Following, the transfection of the cells was conducted using the normalization plasmid pTK-Renilla and Wnt reporter plasmid pGL3-OT (Addgene No. 16558; gifted kindly by Dr. Bert Vogelstein MD, Johns Hopkins University, Baltimore, Md., United States). The cells were incubated for 24 h in Wnt-3a-conditioned medium, control-conditioned medium, or one of two concentrations of AS (50 or 100 μg/mL), following which their lysates were collected and subjected to dual-luciferase activity assay (Promega) performed in triplicates. The values for the firefly luciferase were normalized to those of the *Renilla* luciferase. The Wnt-3a-conditioned medium and control-conditioned medium were synthesized as reported in the literature [20].

2.13. Animals

Athymic nude mice (1–2 months old; female; BALB/*c-nu*) were procured from National Laboratory Animal Center (Nangang District, Taipei City, Taiwan). They were housed in sterile cages and provided with a 12-12 light cycle. The animals were provided with *ad libitum* access to water and rodent chow (Oriental Yeast, Tokyo, Japan). All the experiments were performed according to the China Medical University

Animal Ethics Research Board's guidelines and their approval.

2.14. In vivo anti-metastasis through bioluminescence imaging

The mice were assigned in a random order to one of three groups, each comprising four mice. Bioluminescence imaging indicated that AS inhibited the lung metastasis in live mice injected with MDA-MB-231-luciferase. The body weight of each mouse was recorded every 7 days to monitor drug toxicity. The animals were orally administered AS (100 or 150 mg/kg) for three times/week. Afterward, the MDA-1 × 10^6 MB-231-luciferase cells/100 μL were injected intravenously into the mice, which were anesthetized and intraperitoneally injected with luciferin. The IVIS 200 system was used to image the animal. The photons from each mouse were quantified, and images of the bioluminescent signals emanating from the entire body were acquired. The images' color overlay indicates the luminescence (i.e., photons per second) radiated by the mice. Presented photographs are representative images ($n = 4$). The photon emissions from the entire mouse bodies were quantified. On day 28, all mice were sacrificed, and their lung tissues were excised. A veterinary pathologist examined the mouse organs, including the lungs, kidneys, and liver.

2.15. Histopathological analyses

The isolated lung tissues underwent Western blotting, hematoxylin–eosin (H&E) staining, and immunohistochemical staining. They were fixed using paraformaldehyde (4%) immediately and sectioned, following which was H&E-stained for light microscopy. Thereafter, the nonspecific binding was blocked with (w/v) BSA (1%) for 1 h at room temperature for immunohistochemical staining. Later on, the sections underwent overnight incubation with primary antibody anti-E-cadherin at 4 °C. Following the primary antibody staining, the slides underwent 20-min incubation with a biotinylated secondary antibody (Zymed Laboratories, Calif., United States) at room temperature. Lastly, the slides underwent incubation with an avidin–biotin complex reagent and were stained using 3,3′-diaminobenzidine in accordance per manufacturer instructions (Histostain-Plus Kit, Zymed Laboratories).

2.16. Statistical analyses

The *in vitro* experiment data are shown as the mean ± SD. ANOVA was applied to all study data, and Dunnett's test was applied for pairwise comparisons. Statistical significance for the differences compared with AS-treated cells was set at $*p < 0.05$, $**p < 0.01$, and $***p < 0.001$.

3. Results

3.1. AS inhibits cell invasion and migration in MDA-MB-231 cells

In our earlier study we demonstrated that AS treatment significantly reduced MCF-7, MCF-10A, and MDA-MB-231 cell growth with IC_{50} of 348 μg/mL, 330 μg/mL, and 142 μg/mL, respectively (Chang et al., 2017b). In the present study, our results confirmed that the rate of growth inhibition in human TNBC (MDA-MB-231) cells significantly increases when treated with AS at concentrations of 200 and 400 μg/mL, as shown in Fig. 1A. Hence, a non-cytotoxic AS concentrations in the range 25–100 μg/mL was employed to assess its anti-metastatic and anti-EMT effects on MDA-MB-231 cells.

We observed the impact of AS with concentrations varying from 25 to 100 μg/mL for 12 and 24 h on MDA-MB-231 cell migration using *in vitro* wound-closure assay. It was noted that AS was found to enhance the closure of the wounded area dose-dependently (Fig. 1B and C). Subsequently, AS' ability to inhibit MDA-MB-231 cell invasion was measured through the use of BD Matrigel chamber, as noticed AS treatment (24 h) significantly reduced MDA-MB-231 cell invasion dose-dependently, especially at AS concentrations of 75 and 100 μg/mL (Fig. 1D and E).

3.2. AS downregulated expression of MMPs, uPA, uPAR, and VEGF

Treating MDA-MB-231 cells with AS resulted in remarkable decreases in uPA, uPAR, and MMP-9 protein expression (Fig. 2A). As observed in the Western blot analysis VEGF expression was downregulated following AS treatment (Fig. 2A). The supernatant was gathered and investigated for uPA and MMP-9 effects through gelatin zymography assay and it was observed that AS, dose-dependently reduced MMP-9 and uPA activity in MDA-MB-231 cells (Fig. 2B). Correspondingly, MMP-9 mRNA's gene expression pattern was suppressed by AS in MDA-MB-231 with concentrations 25, 50, 75 and 100 μg/mL (Fig. 2C). In effect, AS had anti-migratory and anti-invasive effects on MDA-MB-231 cells.

3.3. AS attenuated NFκB and PI3K/AKT activation

The PI3K/AKT and NFκB, a family of transcription factors, play key roles in enhancing cancer cell invasiveness. Our results indicated that luciferase reporter assay quantified NFκB activity as high in the control group; however, it decreased dose-dependently in AS-treated cells (Fig. 2D). The immunofluorescence assay indicated that AS dose-dependently decreased the nuclear p65 protein levels relative to the control group, as shown in Fig. 2E. This hypothesis was evaluated while observing the effect of AS on PI3K and AKT phosphorylation. Moreover, AS treatment substantially decreased p-AKT and p-PI3K expression and significantly increased the total PI3K time-dependently (Fig. 2F). A dose dependent inhibition of AKT phosphorylation was observed with AS treatment, while in comparison with the control group (Fig. 2G). The results indicated AS treatment suppressed the migratory and invasive abilities of MDA-MB-231 cells, and these abilities were largely mediated via the PI3K/AKT/NFκB signaling pathway.

3.4. AS reversed EMT through downregulation of mesenchymal marker proteins N-cadherin, Vimentin, twist, and slug and epithelial marker protein E-cadherin upregulation

The role of AS on the morphology of MDA-MB-231 cells was observed. Incubating MDA-MB-231 cells for 24 h with AS concentrations 25–100 μg/mL, resulted in distinct morphological changes such as fibroblastic to epithelial phenotypic changes compared with the control group (Fig. 3A). Following, AS treatment dose-dependently increased E-cadherin expression while in turn reducing N-cadherin expression in MDA-MB-231 cells, as depicted in Fig. 3B. For further confirmation to the above result (Fig. 3B) the mRNA expression level for E-cadherin and N-cadherin was performed. The results suggest that AS dose-dependently improved the mRNA expression of E-cadherin and reduced the mRNA expression of N-cadherin, when treated for a period of 24 h (Fig. 3C). Reduced expression of Vimentin, Twist, and Slug expression in MDA-MB-231 cells were observed when treated with AS (Fig. 3D).

3.5. AS suppressed the Smad3 signaling pathways

MDA-MB-231 cells were subjected to 24 h AS (25–100 μg/mL) treatment and were subsequently incubated with the relevant Smad3 and Smad2 antibodies. Smad3 and Smad2 phosphorylation occurred after 24-h AS treatment (Fig. 3E). The phosphorylation of Ser465/467 residue of Smad3 was observed, whereas, in the total Smad3 protein there was no significant change (Fig. 3E). However, phosphorylation of Smad2 was unaffected by AS (100 μg/mL), and significant variations were not recorded in the total Smad2 protein (Fig. 3E). The luciferase reporter assay results indicated that in addition to altering the phosphorylation, AS treatment at varying concentrations (25–100 μg/mL) for 24 h, significantly reduced the Smad3 transcriptional activity dose-

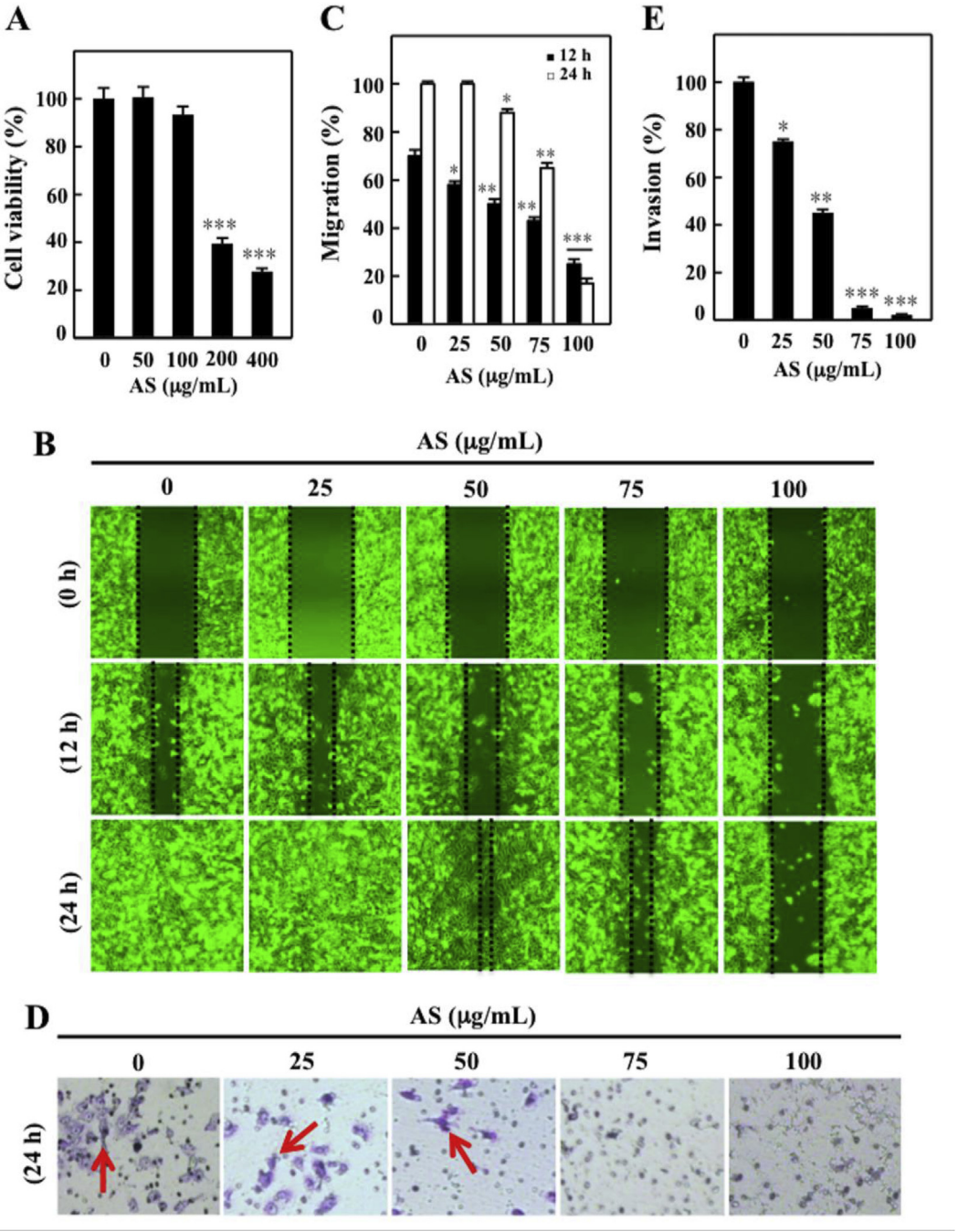

Fig. 1. ***Antrodia salmonea*** **(AS) suppresses the invasion and migration of triple-negative breast cancer (MDA-MB-231) cells.** (A) 24-h treatment of cells with increasing AS concentrations (50–400 μg/mL) or vehicle alone (PBS) using MTT assay. (B–C) Migration assay (D–E) For the Invasion assay, the invasiveness was measured by tallying the cells in 3 microscopic fields per sample. The findings are illustrated as the mean ± SD for 3 independent assays. $*p < 0.05$; $**p < 0.01$; $***p < 0.001$ relative to the untreated cells were set as the significance levels.

dependently, whereas significant changes were not observed in the Smad2 transcriptional activity (Fig. 3F and G). Overall, these results indicated that AS inhibits EMT by restoring E-cadherin and altering other EMT marker proteins in MDA-MB-231 cells.

3.6. AS dowregulated the β-catenin pathways and upregulated GSK3β expression in MDA-MB-231

To determine whether AS modulated Wnt's transcriptional activity in mouse embryonic carcinoma P19 cells, the luciferase reporter system was employed in this study. As Fig. 4A shows, treatment with AS significantly reduced the Wnt reporter activity dose-dependently. To determine whether AS modulated β-catenin's transcriptional activity in MDA-MB-231, we employed the TOP/FOP luciferase reporter system. As Fig. 4B shows, AS dose-dependently and significantly reduced the luciferase activity in TOP reporter vector–transfected cells, whereas negative control FOP reporter vector–transfected cells were unaffected. Therefore, we also ascertained AS′ effect on β-catenin phosphorylation. The result indicated that treatment with AS inhibited p-β-catenin accumulation in the nucleus and increased p-β-catenin expression in the cytoplasmic fraction (Fig. 4C). Similar results were noted in the immunofluorescence assay, which indicated that AS suppressed the expression of nuclear β-catenin in MDA-MB-231 cells (Fig. 4D). These findings suggest that AS antagonized the Wnt pathway through the

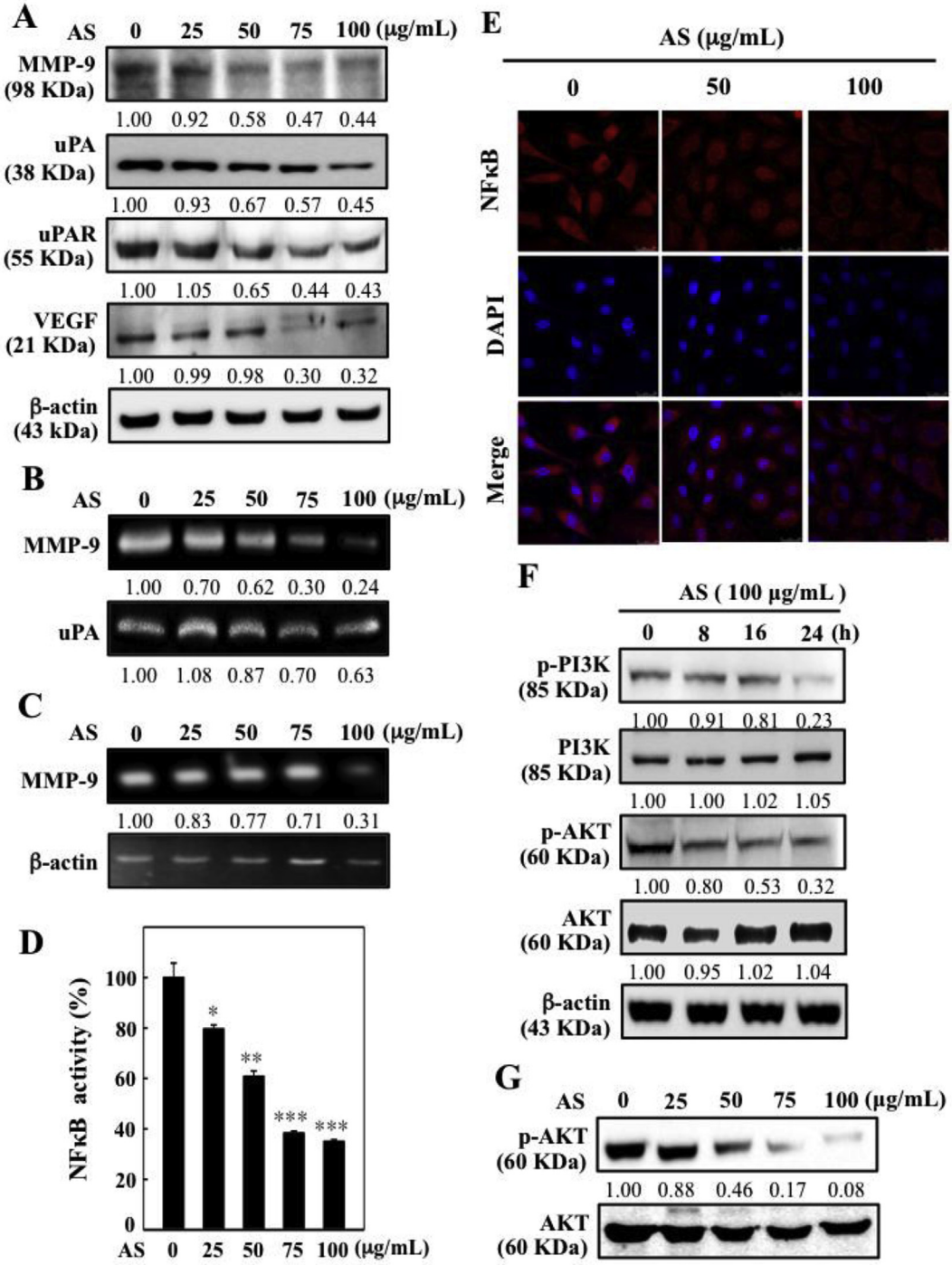

Fig. 2. AS modulates metastasis-related activity and protein expression in MDA-MB-231 cells. (A) AS inhibits metastasis-related proteins. AS induces uPA, uPAR, VEGF, and MMP-9 protein downregulation. Additionally, Western blotting was conducted, with β-actin being the internal control. Relative deviations in the protein bands were ascertained through densitometry, in which the control was set at 100%. (B) The MD-MB-231 cell derived medium that underwent AS treatment was subjected to gelatin zymography. These proteins activities were then quantified through densitometry. (C) The total RNA underwent RT-PCR with one-step RT-PCR master mix and GAPDH gene was used as internal control. (D) Luciferase assay of NFκB promoters. (E) Immunofluorescence staining revealing the variations of NFκB (p65). (F) The PI3K/AKT signaling pathway is inhibited by treatment with AS in MDA-MB-231 cells. (G) PI3K and AKT phosphorylation were evaluated through immunoblotting. The levels of the cell lysate indicated proteins were analyzed with specific antibodies; for sample loading, β-actin was used as internal control.

induction of nuclear β-catenin degradation and indicated that treatment with AS suppressed the expression of nuclear β-catenin in MDA-MB-231 cells. Notably, we determined that AS (25–100 μg/mL) induced GSK3β expression in MDA-MB-231 significantly (Fig. 4E). Moreover, AS treatment inhibited the levels of phosphorylated GSK3β dose-dependently as compared to the control group (Fig. 4E). Overall, we summarize that GSK3β likely plays a role in the AS-induced degradation of β-catenin in MDA-MB-231.

3.7. AS inhibits metastasis and EMT in TGF-β1-stimulated non-tumorigenic MCF-10A cells

TGF-β1-stimulated MCF-10A cells underwent 24-h treatment with increasing AS concentrations (50–400 μg/mL). Relatively more

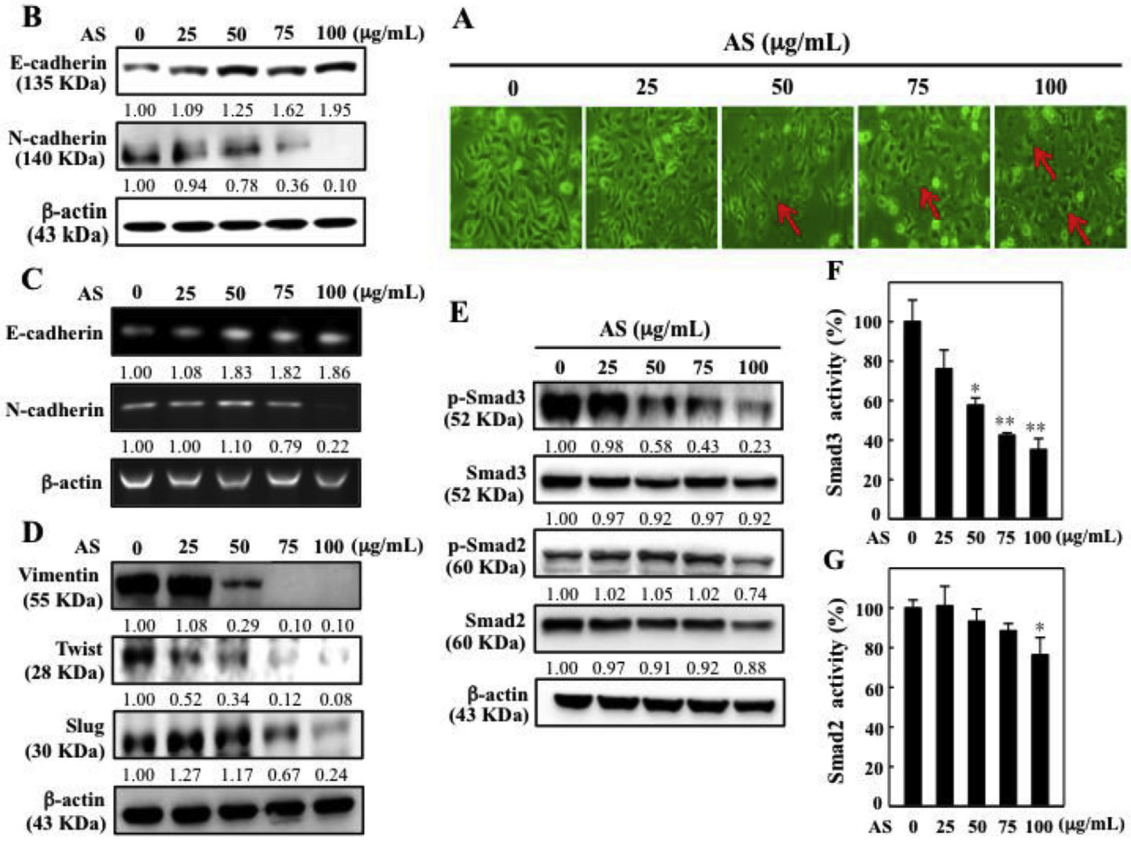

Fig. 3. AS inhibits the epithelial-mesenchymal transition (EMT) by downregulating the mesenchymal marker N-cadherin and upregulating the epithelial marker E-cadherin in MDA-MB-231 cells. (A) Changes in the morphology of MDA-MB-231 cells were characterized through phase-contrast microscopy (magnification: 200×). (B) E-cadherin and N-cadherin immunoblot analysis: Densitometry was used to characterize the relative variations in the protein bands; the control was set to 1.00-fold, as noted below the gel data. (C) The total RNA of E-cadherin and N-cadherin underwent RT-PCR with one-step RT-PCR master mix. The GAPDH gene was an internal control. (D) The levels of total proteins in whole-cell lysates were ascertained through Western blotting. (E) Western blotting of Phosphorylated Smad3 (p-Smad3) and Smad2 (p-Smad2) levels were evaluated using phosphorylation-specific antibodies. β-actin was the internal control. The relative change in the protein bands was ascertained through densitometry; the control was set to 1-fold. (F–G) The transcriptional activity of Smad3 (pGL3-SBE4-Luc) (F) and Smad2 (3 TP-Luc) (G) was monitored using luciferase reporter assays. The data are recorded as the mean ± SD of 3 separate assays. $^{*}p < 0.05$; $^{**}p < 0.01$; $^{***}p < 0.001$ relative to the control were deemed significant.

inhibition of cell growth was observed at 200 and 400 μg/mL of AS (Fig. 5A). Additionally, we examined the impact of AS on the TGF-β1-induced the stimulation of uPA and MMP-9 activity. The gelatin zymography assay revealed that AS pretreatment attenuated the TGF-β1-induced uPA and MMP-9 activity in the TGF-β1-stimulated MCF-10A cells (Fig. 5B). However, AS pretreatment attenuated MMP-9, uPA, VEGF, and Slug expression induced by TGF-β1 (Fig. 5C).

3.8. AS attenuated lung metastasis in BALB/c-nu mice

We employed bioluminescence imaging to analyze the anti-metastatic effects of intraperitoneal administration of AS *in vivo* in live BALB/c-nu mice. All animals appeared healthy, and no adverse effects were observed after treatment with either 100 or 150 mg/kg of AS (Fig. 6A). After incubation with 100 or 150 mg/kg of AS, bioluminescence imaging revealed a significant reduction in the tumor metastasis to the lungs in the AS-treated groups relative to the vehicle-treated groups (Fig. 6B). The differences in lung tumor burden were quantified by ascertaining the photon counts; they were expressed as tumor burden in relation to the photon counts prior to the initial therapeutic injection (Fig. 6C). Dunnett's test indicated that the tumor burden was inhibited significantly in the AS group relative to the vehicle-treated control (Fig. 6C). These results indicated that AS can inhibit MDA-MB-231 lung metastasis. Histopathological analysis using H&E staining revealed multiple tumor distributions in the lung tissues of the vehicle-treated control group, and the tumors exhibited a high degree of mitosis (Fig. 7A). The AS treatment groups (100 and 150 mg/kg) possessed few tumors and low mitotic rates (Fig. 7A), which indicated that AS can inhibit tumor lung metastasis and proliferation. Furthermore, to confirm the mechanism through which AS attenuates tumor lung metastasis, E-cadherin was assessed through immunohistochemistry in the AS-treated (100 and 150 mg/kg) groups. The results indicated that treatment with AS increased E-cadherin expression relative to the control group (Fig. 7B and C). Overall, these findings suggest that AS attenuated metastasis and EMT in MDA-MB-231–cell xenografted nude mice.

4. Discussion

TNBC remains correlated with short survival and high recurrence rates. Although the rate of metastasis of TNBC was comparable to other breast cancer subtypes, patients with TNBC are four times more likely to develop visceral metastases than patients with non-TNBC subtypes (Tseng et al., 2013). Further elucidation of the processes regulating TNBC growth and metastasis and the driving factors of these processes could result in new therapeutic targets and approaches for high-risk patients.

Antrodia. salmonea is considered as one of the edible mushrooms that are endemic to Taiwan and previously named as *Cu.konishii* (Chang and Chou, 2004). Previous various studies using IR, NMR and MS,

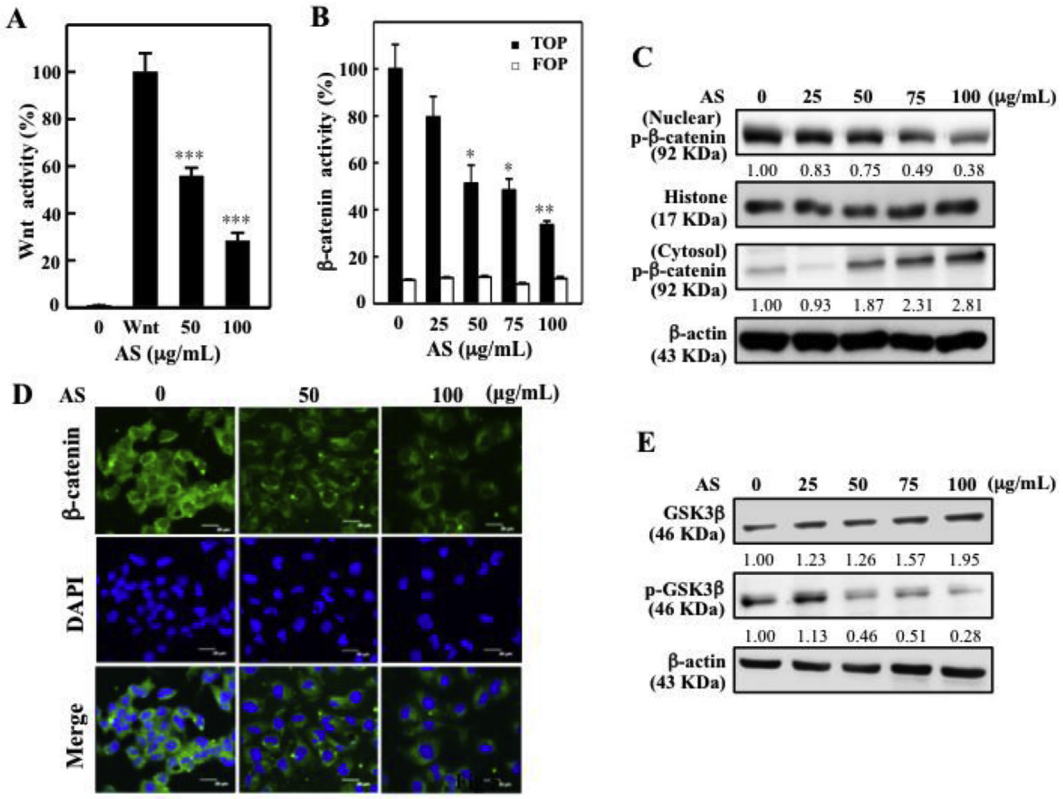

Fig. 4. AS suppresses the Wnt/β-catenin signaling pathways. (A) The cells underwent transfection with the normalization plasmid pTK-Renilla and the Wnt reporter plasmid pGL3-OT. (B) Transient transfection with the FOP*Flash* or TOP*Flash* plasmids using lipofectamine. The relative β-catenin activity was measured by dividing the treated cells' relative luciferase units (RLUs) by the untreated cells' RLUs. (C) β-catenin levels in the cytoplasmic and nuclear fraction were measured through Western blotting. β-actin and Histone H3 served as internal loading controls. The photomicrographs derive from one (out of 3) representative experiment. (D) Immunofluorescence assay was conducted to ascertain MDA-MB-231 cell β-catenin expression. (E). GSK3β and p-GSK3β′s total protein levels in whole cells ascertained using Western blotting. We present the results as the mean ± SD for three independent assays. $*p < 0.05$; $**p < 0.01$; $***p < 0.001$ relative to the control were deemed significant.

denoted the presence of compounds like candinadiene, germacrene D, 2-methoxy-6-methyl-p-benzoquinone, isolongifolene, α-cedrene, 1-octen-3-ol, D-limonene, candinadiene as well as eburcoic acid, fomefficinic acid and pyrroledione in *A. salmonea* (Shen et al., 2008; Chen et al., 2016). Of these, 2-methoxy-6-methyl-p-benzoquinone, isolated from AS fruit bodies, demonstrated potent anticancer effects against KB, H2058, and HepG2 cell lines (Shen et al., 2008). Our earlier works have revealed that fermented AS culture broth exhibits numerous pharmacological effects, for example, anticancer activity (Chang et al., 2017b; Hseu et al., 2014a, 2014b). The results of HPLC analysis indicated that AS comprises approximately 11.6% of 2,4-dimethoxy-6-methylbenzene-1,3-diol, which was confirmed by the obtained NMR and LC-MS spectral data in previous studies (Hseu et al., 2014a; Shen et al., 2008).

The current work determined that AS significantly suppressed metastasis as well as the EMT ability of human TNBC (MDA-MB-231) cells. To best of our knowledge, this study is the first to examine AS′ inhibitory effects on the invasion and migration abilities of MDA-MB-231; our findings validate and extend AS's anti-metastatic action. Previously, we demonstrated that *Antrodia camphorata* inhibited EMT consistently by downregulating the mesenchymal and upregulating the epithelial marker proteins and potentially suppressed migration and invasion by downregulating the PI3K/AKT/NFκB signaling pathways in human colon cancer lines (Hseu et al., 2017). These data suggest AS acts as an anti-metastatic and anti-EMT agent in TNBC cells. Furthermore, they suggested the molecular signaling pathways that play a role in this phenomenon.

Cancer cells in order to be invasive, they have to transverse vessel walls and to facilitate the process they secrete uPA and MMPs which are crucial in cancer cell metastasis and invasion. The metastatic potential and tumor cell growth depend on the MMP levels, as was demonstrated in tumor cell models (Deryugina and Quigley, 2015). As revealed in the current work, AS may reduce the protein levels or activity of proteins relating to tumor metastasis, for example, uPA, uPAR, and MMP-9, in MDA-MB-231 cells, which suggests that AS is a potential antimetastasis agent in breast cancer cells. Moreover, AS was found to inhibit VEGF (a primary angiogenic cytokine) expression in MDA-MB-231 cells. Changed epithelial cells may be the strongest source of VEGF release in myriad cancers. VEGF expression is linked to aggressive tumor behavior and increased angiogenesis (Keyhani et al., 2013). AS' inhibitory effects on the expression of VEGF in breast cancer cells is likely thus a vital pathway in neovascularization regulation in human breast tumors, which may contribute to controlling tumor progression and growth.

NFκB activation leads to the downregulation of the PI3K/AKT pathway, which is involved in numerous pathological processes, like cancer cell adhesion, inflammation, angiogenesis, invasion, and metastasis. Inhibition of NFκB activation suppresses uPA, VEGF, and MMPs and tumor metastasis (Du and Geller, 2010). The present study determined that AS inhibits constitutively activated NFκB's transcriptional activity. The suppression of the NFκB activity could block tumor promotion, metastasis, and initiation as well as block any factors binding to these regulatory elements. This approach appears to be suitable for inhibiting uPA, MMPs, and VEGF expression. Data from the current work suggested that inhibition of MDA-MB-231 cell invasiveness mediated by AS may be partly mediated through the suppressing of uPA, VEGF, and MMPs expression through modulation of the NFκB signaling pathways. Osaki et al. (2004) and Xiang et al. (2016) have both recognized the PI3K/AKT signaling pathways as well as their downstream factors as primary regulators of cell life cycle, namely, cell

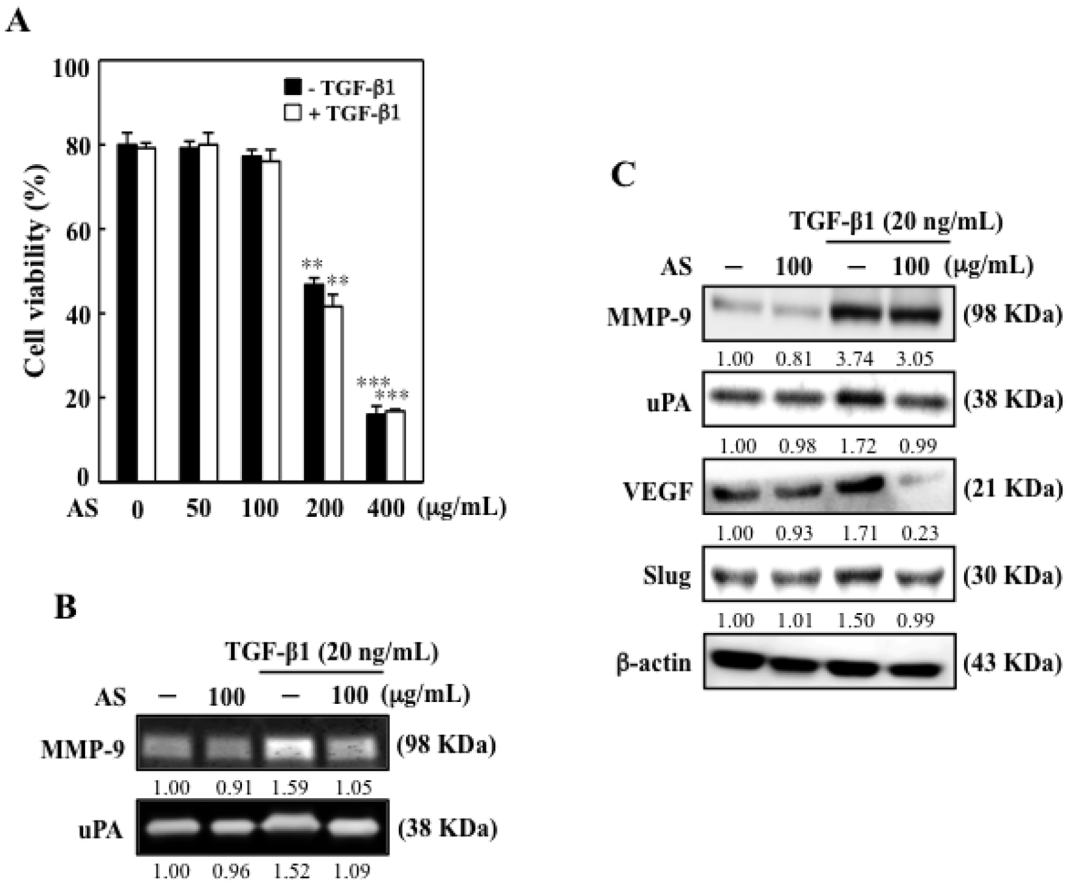

Fig. 5. AS inhibits the TGF-β1-induced metastasis and EMT in MCF-10A cells. (A) MTT assay after treatment with or without TGF-β1 (20 ng/mL), or with the combination of TGF-β1 and AS (50–400 μg/mL) for 24 h. (B) The inhibition of MMP-9 and uPA activity in conditioned medium from MCF-10A cells after 24 h treatment with or without TGF-β1 (10 ng/mL) or the combination of TGF-β1 and AS (100 μg/mL) was evaluated using gelatin zymography. (C) Western blot after treatment with or without TGF-β1 (10 ng/mL) or the combination of TGF-β1 and AS (100 μg/mL) for 24 h. All of the photomicrographs and histograms shown here are from one of the representative experiment, which were performed in triplicates. The results are presented as the means ± S.D of three independent assays. Significant at $*p < 0.05$; $**p < 0.01$; $***p < 0.001$ compared to untreated control cells.

survival, cell proliferation, cell invasion, and cell migration. In colorectal cancer, for example, PI3K/AKT is constitutively activated, offering an effective target for therapeutic agents (Danielsen et al., 2015). PI3K/AKT is directly targeted by the NFκB transcription factor and was associated with metastasis and invasion in many cancers (Ahmad et al., 2013). The present study determined that AS treatment significantly reduces NFκB protein expression, which suggests that AS negatively regulates NFκB activity, possibly through influencing the PI3K/AKT signaling pathway's activity within breast cancer cells. Thus, we speculate that PI3K/AKT/NFκB inhibition accounts for AS′ anti-metastatic effects in TNBCs.

EMT is one of the crucial survival mechanisms of cancer cells. Changes in cadherin expression may be crucial in EMT and cellular motility processes. Some malignant tumors, especially undifferentiated tumors that are metastatic, are largely negative for E-cadherin; however, they are sometimes positive for N-cadherin. This dichotomy is known as the cadherin switch. Non-epithelial cadherin's, an example of which is N-cadherin, trigger a mesenchymal-scattered phenotype that is correlated with decreased E-cadherin in squamous epithelial cells (Araki et al., 2011). This cadherin switch is correlated with the migratory and invasive properties of breast cancer cells. Andrews et al. (2012) described the downregulation of E-cadherin and upregulation of N-cadherin in breast cancer. This pattern was observed in the present study, in which AS treatment induced E-cadherin and suppressed N-cadherin. E-cadherin is an adherens junction protein and is expressed in healthy breast tissue. Additionally, it is valuable as a phenotypic marker in breast cancers (Singhai et al., 2011). E-cadherin loss stimulates EMT, which is responsible for cells' progression to the metastatic state. The specific mechanism to which E-cadherin inactivation in cancer cells is attributable remains unclear; nevertheless, transcriptional-level alterations may explain its downregulation (Thiery, 2002). One study on Withaferin A found that restoration of the transcription and protein levels of E-cadherin was correlated with cell proliferation and metastasis inhibition of breast cancer cells (Lee et al., 2015). In our study, the AS-induced restoration of the transcription and protein levels of E-cadherin was demonstrated to inhibit the progression of metastasis and EMT in TNBC. Furthermore, the *in vivo* experiment confirmed that AS increased E-cadherin expression and suppressed breast cancer metastasis to the lungs. A family of master zinc finger regulatory proteins, including Twist, Slug, and Vimentin, directly regulates EMT (Wu et al., 2010). Vimentin maintains cellular integrity, while Twist and Slug are transcriptional factors that regulate E-cadherin (Wu et al., 2010). Numerous studies have elucidated the key roles played by signaling pathways that result in the transcriptional repression of the epithelial phenotype by such factors that serve as critical regulators of EMT in promoting the metastasis of prostate cancer (Wu et al., 2010). In our current study, it was noted that AS suppressed EMT through downregulating the transcription of the proteins Vimentin, Twist, and Slug. This could delay the metastasis of human breast cancer cells. Smad3 is a critical regulatory factor of the TGF-β1 pathway, which is crucial for the development of metastatic breast cancer and many other cancers (Walker et al., 2010). Furthermore, we determined that the MMP-9 levels, which are an indicator of the invasiveness of cancer cells, correlated with the phosphorylated Smad3 levels in the breast cancer cells.

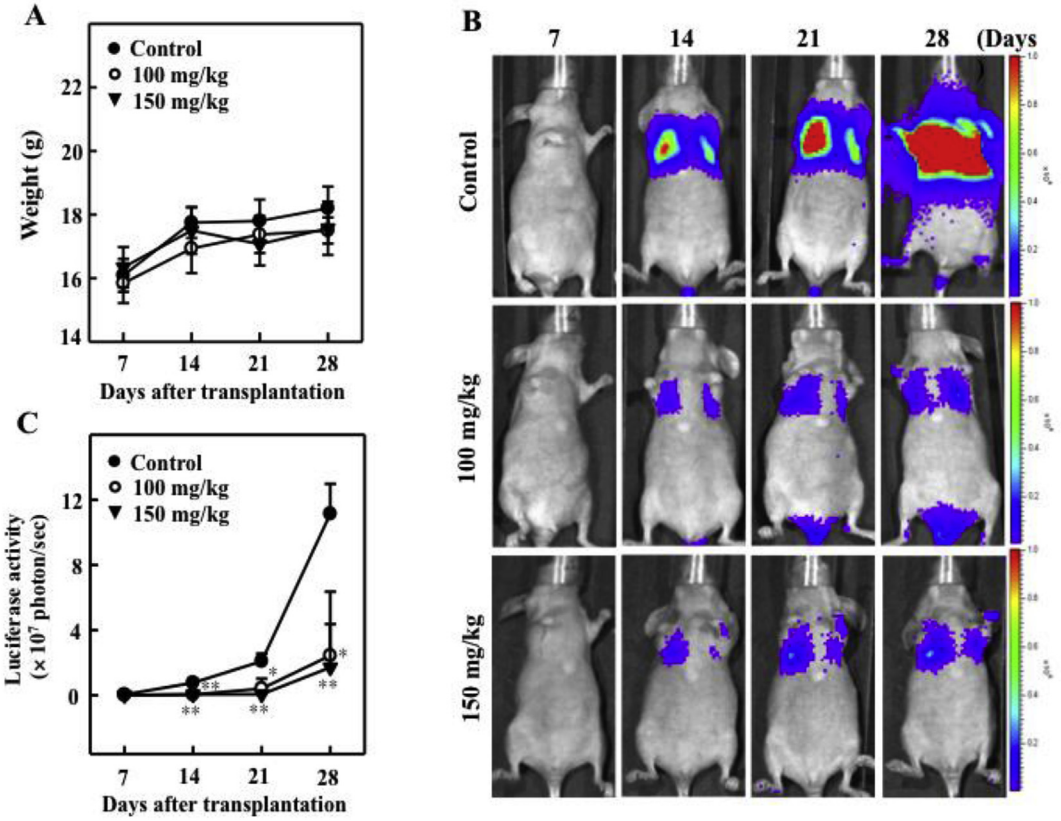

Fig. 6. *In vivo* AS treatment for antimetastatic activity. Inhibition of lung metastasis in live MDA-MB-231 luciferase injected mice, demonstrated by bioluminescence imaging. The mice underwent AS (100 or 150 mg/kg) or vehicle only (control) treatment and were subsequently intravenously injected with the MDA-MB-231-luciferase cells (1×10^6 cells per well). On day 0, the cells were intravenously implanted into the nude mice. (A) Measurement of mouse body weighted every 7 days for 28 days, presented the results as the mean ± SE (n = 4). (B–C) Bioluminescence imaging performed for every 7 days for 28 days. The color overlay represents the animal's luminescence (photons/s) emissions as indicated by the color scales. The photographs are representative images (n = 4). Data are shown as the mean ± SD of 3 separate assays. $^*p < 0.05$; $^{**}p < 0.01$; $^{***}p < 0.001$ relative to the control were deemed significant. (For interpretation of the references to color in this figure legend, the reader is referred to the Web version of this article.)

AS enhanced the suppression of Smad3 phosphorylation and demonstrated an anti-metastatic impact on breast cancer cells. Overall, our data suggested that AS inhibits Smad3 signaling during cancer metastasis.

E-cadherin/β-catenin suppression may contribute to tumor invasion and metastasis (Sommers et al., 1994). E-cadherin has a critical role in β-catenin function and stabilization has been evidenced in the literature. On supression of E-cadherin, β-catenin may disassociate from E-cadherin/β-catenin complexes, becoming free to translocate to the nucleus. Furthermore, β-catenin binds to the TCF/LEF-1 element and, in association with some transcription factors, transcriptionally activates numerous promigratory genes for EMT (Gonzalez-Moles et al., 2014). This indicates that AS restores the E-cadherin/β-catenin complex formation in MDA-MB-231, further impeding the nuclear transport of β-catenin, which in turn increases E-cadherin expression by inhibiting its master regulator, including Vimentin, Twist, and Slug. The current work revealed that AS' anti-EMT effects are correlated with the regulation of the formation of the E-cadherin/β-catenin complex.

This study demonstrated AS anti-metastatic and anti-EMT capabilities while proposing a potential mechanism in non-tumorigenic MCF-10A cells that are TGF-β1-induced. TGF-β1 enhances tumor progression by stimulating the complex process of EMT. TGF1-β-induced EMT which is marked by the loss of junctional E-cadherin localization, acquisition of fibroblastic morphology, increased cellular motility, and the presence of stress fibers (Bhowmick et al., 2001). AS beneficial effects were demonstrated by the downregulation of uPA and MMP-9 activities in TGF-β1-induced activation. Additionally, this compound altered the expression of VEGF and Slug, which are key molecular events in the suppression of TGF-β1-engendered metastasis and EMT in TGF-β1-stimulated MCF-10A cells.

We further assume that AS metabolizes elements of the culture media and enhances the release of several active constituents during fermentation in submerged culture. Such biochemical processes may contribute to the anti-metastatic and anti-EMT activities in human TNBC cells. Nevertheless, future studies are necessary for identification and verification of individual bioactive compounds responsible for AS' anticancer effects.

5. Conclusions

In short, the current study demonstrated the *in vivo* and *in vitro* anti-EMT and anti-metastatic activities of *Antrodia salmonea* against human TNBCs. These activities could have been mediated through the inhibition of NFκB and modulation of Wnt/β-catenin signaling pathways and further research needs to be conducted to clarify the relationship between NF-κβ and Wntβ-catenin when treated with *Antrodia salmonea*. Henceforth, these results provide a new perspective of AS' actions as an inhibitor of metastasis and EMT in human TNBCs.

Competing of financial interest

All authors declared no conflicts of interest to this study.

Acknowledgements

This work was supported by the grants MOST-106-2320-B-039-054-

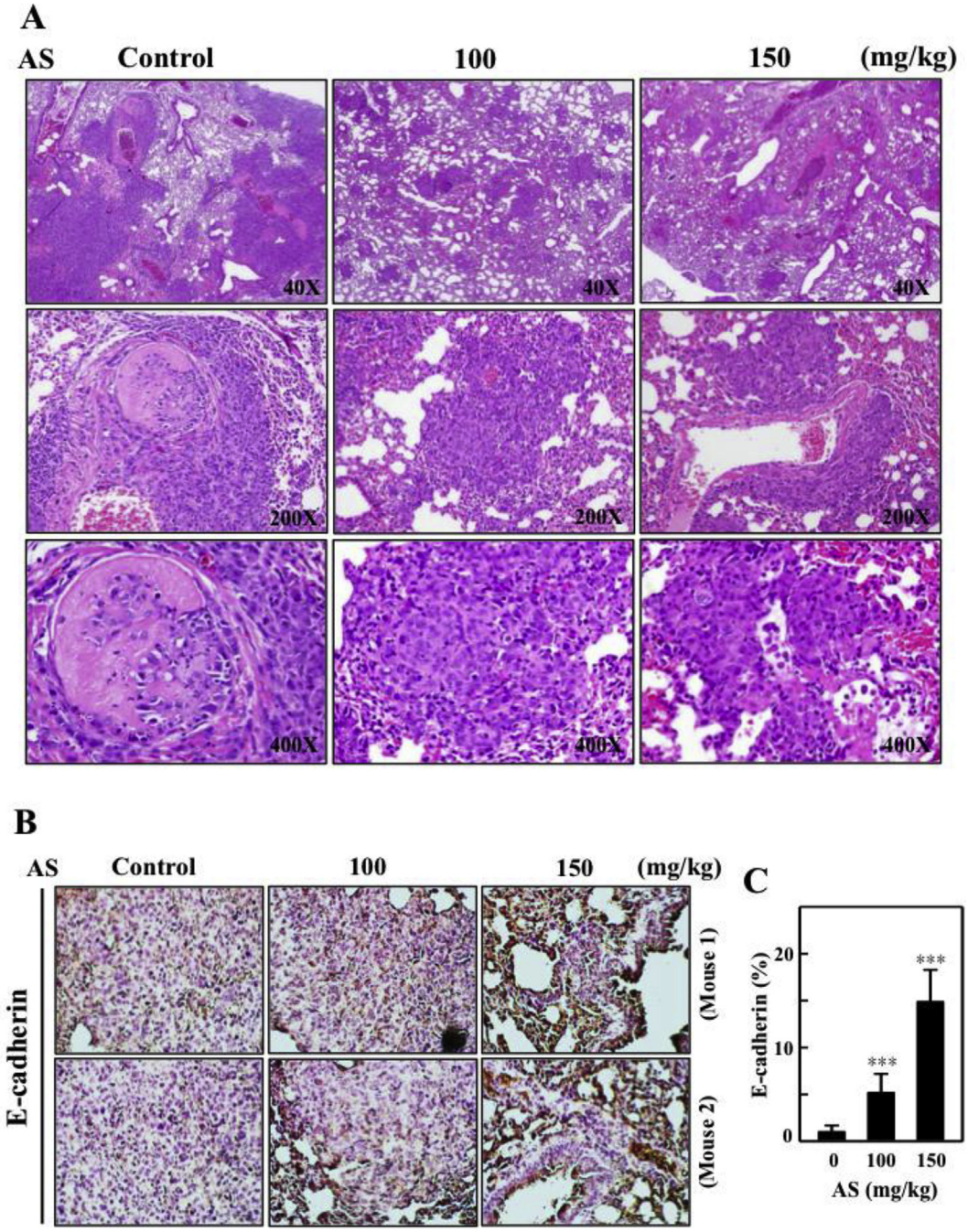

Fig. 7. Inhibition of metastasis to lung tissues by AS in mice injected with MDA-MB-231-luciferase. Lung sections were obtained from animals subjected to AS (100 or 150 mg/kg) treatment and controls. On day 28 after tumor implantation, the mice were killed. Subsequently, the lung tissues were extracted and sectioned. (A) Histochemical analysis of mouse lung sections was performed using light microscopy (magnification: 40×, 200×, and 400×). (B–C) E-cadherin was examined through immunohistochemical staining. The results are the mean ± SE numbers of cells or microscope field (as percentages) for four mice per group. The results are presented as the mean ± SD of three independent assays. $^{*}p < 0.05$; $^{**}p < 0.01$; $^{***}p < 0.001$ relative to the control were deemed significant.

MY3 and MOST-107-2320-B-039-013-MY3 from the Ministry of Science and Technology, Taiwan. This work was financially supported by the "Chinese Medicine Research Center, China Medical University" from The Featured Areas Research Center Program within the framework of the Higher Education Sprout Project by the Ministry of Education in Taiwan (CMRC-CHM-9).

Transparency document

Transparency document related to this article can be found online at https://doi.org/10.1016/j.fct.2018.12.009.

References

Ahmad, A., Biersack, B., Li, Y., Kong, D., Bao, B., Schobert, R., Padhye, S.B., Sarkar, F.H., 2013. Targeted regulation of PI3K/Akt/mTOR/NF-κB signaling by indole compounds and their derivatives: mechanistic details and biological implications for cancer therapy. Anti Cancer Agents Med. Chem. 13, 1002–1013.

Andrews, J.L., Kim, A.C., Hens, J.R., 2012. The role and function of cadherins in the mammary gland. Breast Cancer Res. 14, 203.

Araki, K., Shimura, T., Suzuki, H., Tsutsumi, S., Wada, W., Yajima, T., Kobayahi, T., Kubo, N., Kuwano, H., 2011. E/N-cadherin switch mediates cancer progression via TGF-beta-induced epithelial-to-mesenchymal transition in extrahepatic cholangiocarcinoma. Br. J. Canc. 105, 1885–1893.

Bao, B., Mitrea, C., Wijesinghe, P., Marchetti, L., Girsch, E., Farr, R.L., Boerner, J.L.,

Mohammad, R., Dyson, G., Terlecky, S.R., Bollig-Fischer, A., 2017. Treating triple negative breast cancer cells with erlotinib plus a select antioxidant overcomes drug resistance by targeting cancer cell heterogeneity. Sci. Rep. 7, 44125.
Bhowmick, N.A., Ghiassi, M., Bakin, A., Aakre, M., Lundquist, C.A., Engel, M.E., Arteaga, C.L., Moses, H.L., 2001. Transforming growth factor-beta1 mediates epithelial to mesenchymal transdifferentiation through a RhoA-dependent mechanism. Mol. Biol. Cell 12, 27–36.
Chang, C.T., Hseu, Y.C., Thiyagarajan, V., Huang, H.C., Hsu, L.S., Huang, P.J., Liu, J.Y., Liao, J.W., Yang, H.L., 2017a. *Antrodia salmonea* induces G2 cell-cycle arrest in human triple-negative breast cancer (MDA-MB-231) cells and suppresses tumor growth in athymic nude mice. J. Ethnopharmacol. 196, 9–19.
Chang, C.T., Korivi, M., Huang, H.C., Thiyagarajan, V., Lin, K.Y., Huang, P.J., Liu, J.Y., Hseu, Y.C., Yang, H.L., 2017b. Inhibition of ROS production, autophagy or apoptosis signaling reversed the anticancer properties of *Antrodia salmonea* in triple-negative breast cancer (MDA-MB-231) cells. Food Chem. Toxicol. 103, 1–17.
Chang, T.T., Chou, W.N., 2004. Antrodia cinnamomea reconsidered and A. salmonea sp. nov. on Cunninghamia konishii in Taiwan. Bot. Bull. Acad. Sin. 45, 347–352.
Chen, C.Y., Chien, S.C., Tsao, N.W., Lai, C.S., Wang, Y.Y., Hsiao, W.W., Chu, F.H., Kuo, Y.H., Wang, S.Y., 2016. Metabolite profiling and comparison of bioactivity in Antrodia cinnamomea and Antrodia salmonea fruiting bodies. Planta Med. 82 (3), 244–249.
Danielsen, S.A., Eide, P.W., Nesbakken, A., Guren, T., Leithe, E., Lothe, R.A., 2015. Portrait of the PI3K/AKT pathway in colorectal cancer. Biochim. Biophys. Acta 1855, 104–121.
Deryugina, E.I., Quigley, J.P., 2015. Tumor angiogenesis: MMP-mediated induction of intravasation- and metastasis-sustaining neovasculature. Matrix Biol. 44–46, 94–112.
Du, Q., Geller, D.A., 2010. Cross-regulation between Wnt and NF-kappaB signaling pathways. Forum Immunopathol. Dis. Ther. 1, 155–181.
Gonzalez-Moles, M.A., Ruiz-Avila, I., Gil-Montoya, J.A., Plaza-Campillo, J., Scully, C., 2014. beta-catenin in oral cancer: an update on current knowledge. Oral Oncol. 50, 818–824.
Heo, S.H., Choi, Y.J., Ryoo, H.M., Cho, J.Y., 2010. Expression profiling of ETS and MMP factors in VEGF-activated endothelial cells: role of MMP-10 in VEGF-induced angiogenesis. J. Cell. Physiol. 224, 734–742.
Hseu, Y.C., Lee, C.C., Chen, Y.C., Kumar, K.S., Chen, C.S., Tsai, C.T., Huang, H.C., Wang, H.M., Yang, H.L., 2014a. *Antrodia salmonea* in submerged culture exhibits antioxidant activities *in vitro* and protects human erythrocytes and low-density lipoproteins from oxidative modification. Food Chem. Toxicol. 66, 150–157.
Hseu, Y.C., Lee, C.C., Chen, Y.C., Kumar, K.S.J., Chen, C.S., Huang, Y.C., Hsu, L.S., Huang, H.C., Yang, H.L., 2014b. The anti-tumor activity of *Antrodia salmonea* in human promyelocytic leukemia (HL-60) cells is mediated via the induction of G1 cell-cycle arrest and apoptosis *in vitro* or *in vivo*. J. Ethnopharmacol. 153, 499–510.
Hseu, Y.C., Chao, Y.H., Lin, K.Y., Way, T.D., Lin, H.Y., Thiyagarajan, V., Yang, H.L., 2017. *Antrodia camphorata* inhibits metastasis and epithelial-to-mesenchymal transition via the modulation of claudin-1 and Wnt/beta-catenin signaling pathways in human colon cancer cells. J. Ethnopharmacol. 208, 72–83.
Hseu, Y.C., Lee, C.C., Chen, Y.C., Kumar, K.J., Chen, C.S., Huang, Y.C., Hsu, L.S., Huang, H.C., Yang, H.L., 2014c. The anti-tumor activity of *Antrodia salmonea* in human promyelocytic leukemia (HL-60) cells is mediated via the induction of G(1) cell-cycle arrest and apoptosis *in vitro* or *in vivo*. J. Ethnopharmacol. 153, 499–510.
Hseu, Y.C., Lee, C.C., Chen, Y.C., Senthil Kumar, K.J., Chen, C.S., Tsai, C.T., Huang, H.C., Wang, H.M., Yang, H.L., 2014d. *Antrodia salmonea* in submerged culture exhibits antioxidant activities *in vitro* and protects human erythrocytes and low-density lipoproteins from oxidative modification. Food Chem. Toxicol. 66, 150–157.
Isakoff, S.J., 2010. Triple negative breast cancer: role of specific chemotherapy agents. Cancer J. 16 (1), 53–61.
Keyhani, E., Muhammadnejad, A., Behjati, F., Sirati, F., Khodadadi, F., Karimlou, M., Moghaddam, F.A., Pazhoomand, R., 2013. Angiogenesis markers in breast cancer–potentially useful tools for priority setting of anti-angiogenic agents. Asian Pac. J. Cancer Prev. APJCP 14, 7651–7656.
Lee, J., Hahm, E.R., Marcus, A.I., Singh, S.V., 2015. Withaferin A inhibits experimental epithelial-mesenchymal transition in MCF-10A cells and suppresses vimentin protein level *in vivo* in breast tumors. Mol. Carcinog. 54, 417–429.
Maier, H.J., Schmidt-Strassburger, U., Huber, M.A., Wiedemann, E.M., Beug, H., Wirth, T., 2010. NF-kappaB promotes epithelial-mesenchymal transition, migration and invasion of pancreatic carcinoma cells. Cancer Lett. 295, 214–228.
Osaki, M., Oshimura, M., Ito, H., 2004. PI3K-Akt pathway: its functions and alterations in human cancer. Apoptosis 9, 667–676.
Pai, H.C., Chang, L.H., Peng, C.Y., Chang, Y.L., Chen, C.C., Shen, C.C., Teng, C.M., Pan, S.L., 2013. Moscatilin inhibits migration and metastasis of human breast cancer MDA-MB-231 cells through inhibition of Akt and Twist signaling pathway. J. Mol. Med. 91, 347–356.
Sehrawat, A., Singh, S.V., 2011. Benzyl isothiocyanate inhibits epithelial-mesenchymal transition in cultured and xenografted human breast cancer cells. Cancer Prev. Res. 4 (7), 1107–1117.
Shen, C.C., Lin, C.F., Huang, Y.L., Wan, S.T., Chen, C.C., Sheu, S.J., Lin, Y.C., Chen, C.C., 2008. Bioactive components from the mycelium of *Antrodia salmonea*. J. Chin. Chem. Soc. 55, 854–857.
Singhai, R., Patil, V.W., Jaiswal, S.R., Patil, S.D., Tayade, M.B., Patil, A.V., 2011. E-cadherin as a diagnostic biomarker in breast cancer. N. Am. J. Med. Sci. 3, 227–233.
Sommers, C.L., Gelmann, E.P., Kemler, R., Cowin, P., Byers, S.W., 1994. Alterations in beta-catenin phosphorylation and plakoglobin expression in human breast cancer cells. Cancer Res. 54, 3544–3552.
Tang, J.L., Liu, B.Y., Ma, K.W., 2008. Traditional Chinese medicine. Lancet 372, 1938–1940.
Thiery, J.P., 2002. Epithelial-mesenchymal transitions in tumour progression. Nat. Rev. Canc. 2, 442–454.
Tsai, Z.T.,L.S., 1985. The Use and the Effect of *Ganoderma*. San Yun Press, Taichung, Taiwan.
Tseng, L.M., Hsu, N.C., Chen, S.C., Lu, Y.S., Lin, C.H., Chang, D.Y., Li, H., Lin, Y.C., Chang, H.K., Chao, T.C., Ouyang, F., Hou, M.F., 2013. Distant metastasis in triple-negative breast cancer. Neoplasma 60, 290–294.
Wahba, H.A., El-Hadaad, H.A., 2015. Current approaches in treatment of triple-negative breast cancer. Cancer. Biol. Med. 12 (2), 106–116.
Walker, L.C., Fredericksen, Z.S., Wang, X., Tarrell, R., Pankratz, V.S., Lindor, N.M., Beesley, J., Healey, S., Chen, X., kConFab, Stoppa-Lyonnet, D., Tirapo, C., Giraud, S., Mazoyer, S., Muller, D., Fricker, J.P., Delnatte, C., Collaborators, G.S., Schmutzler, R.K., Wappenschmidt, B., Engel, C., Schonbuchner, I., Deissler, H., Meindl, A., Hogervorst, F.B., Verheus, M., Hooning, M.J., van den Ouweland, A.M., Nelen, M.R., Ausems, M.G., Aalfs, C.M., van Asperen, C.J., Devilee, P., Gerrits, M.M., Waisfisz, Q., Hebon Szabo, C.I., ModSqua, D., Easton, D.F., Peock, S., Cook, M., Oliver, C.T., Frost, D., Harrington, P., Evans, D.G., Lalloo, F., Eeles, R., Izatt, L., Chu, C., Davidson, R., Eccles, D., Ong, K.R., Cook, J., Embrace Rebbeck, T., Nathanson, K.L., Domchek, S.M., Singer, C.F., Gschwantler-Kaulich, D., Dressler, A.C., Pfeiler, G., Godwin, A.K., Heikkinen, T., Nevanlinna, H., Agnarsson, B.A., Caligo, M.A., Olsson, H., Kristoffersson, U., Liljegren, A., Arver, B., Karlsson, P., Melin, B., Swe, B., Sinilnikova, O.M., McGuffog, L., Antoniou, A.C., Chenevix-Trench, G., Spurdle, A.B., Couch, F.J., 2010. Evidence for SMAD3 as a modifier of breast cancer risk in BRCA2 mutation carriers. Breast Cancer Res. 12, R102.
Wang, H., Wang, H.S., Zhou, B.H., Li, C.L., Zhang, F., Wang, X.F., Zhang, G., Bu, X.Z., Cai, S.H., Du, J., 2013. Epithelial-mesenchymal transition (EMT) induced by TNF-alpha requires AKT/GSK-3beta-mediated stabilization of snail in colorectal cancer. PLoS One 8, e56664.
Wang, Q., Cheng, Y., Wang, Y., Fan, Y., Li, C., Zhang, Y., Wang, Y., Dong, Q., Ma, Y., Teng, Y.E., Qu, X., Liu, Y., 2017. Tamoxifen reverses epithelial-mesenchymal transition by demethylating miR-200c in triple-negative breast cancer cells. BMC Canc. 17, 492.
Wu, K., Zeng, J., Li, L., Fan, J., Zhang, D., Xue, Y., Zhu, G., Yang, L., Wang, X., He, D., 2010. Silibinin reverses epithelial-to-mesenchymal transition in metastatic prostate cancer cells by targeting transcription factors. Oncol. Rep. 23, 1545–1552.
Xiang, T., Yu, F., Fei, R., Qian, J., Chen, W., 2016. CHRNA7 inhibits cell invasion and metastasis of LoVo human colorectal cancer cells through PI3K/Akt signaling. Oncol. Rep. 35, 999–1005.
Yang, H.L., Chang, H.C., Lin, S.W., Senthil Kumar, K.J., Liao, C.H., Wang, H.M., Lin, K.Y., Hseu, Y.C., 2014. *Antrodia salmonea* inhibits TNF-alpha-induced angiogenesis and atherogenesis in human endothelial cells through the down-regulation of NF-kappaB and up-regulation of Nrf2 signaling pathways. J. Ethnopharmacol. 151, 394–406.
Yang, H.L., Lin, S.W., Lee, C.C., Lin, K.Y., Liao, C.H., Yang, T.Y., Wang, H.M., Huang, H.C., Wu, C.R., Hseu, Y.C., 2015. Induction of Nrf2-mediated genes by *Antrodia salmonea* inhibits ROS generation and inflammatory effects in lipopolysaccharide-stimulated RAW264.7 macrophages. Food. Funct. 6, 230–241.
Yao, H., Ashihara, E., Maekawa, T., 2011. Targeting the Wnt/beta-catenin signaling pathway in human cancers. Expert Opin. Ther. Targets 15, 873–887.